Psychophysiological dynamics of emotional reactivity: Interindividual reactivity characterization and prediction by a machine learning approach

Damien Claverie, Roman Rutka, Vaida Verhoef, Frédéric Canini, Pascal Hot, Sonia Pellissier

Title: Psychophysiological dynamics of emotional reactivity: interindividual reactivity characterization and prediction by a machine learning approach

Authors: Damien Claverie[1, *], Roman Rutka[2,3, *], Vaida Verhoef[3], Frédéric Canini[1,4], Pascal Hot[3,5], Sonia Pellissier[2]

Affiliations

*: equivalent contribution

[1]: Département Neurosciences & Contraintes Opérationnelles, Institut de Recherche Biomédicale des Armées (IRBA), Brétigny-sur-Orge, France.

[2]: LIP/PC2S, Université Savoie Mont Blanc and Université Grenoble Alpes, Chambéry, France.

[3]: LPNC-UMR CNRS 5105, Université Savoie Mont Blanc, UFR LLSH, Chambéry, France.

[4]: Ecole du Val de Grâce, Paris, France.

[5]: Institut Universitaire de France.

Corresponding author:

Damien Claverie: claveriedamien@hotmail.com

Phone: +33662570900

Highlights:

- Cross-correlations between RR and tonic electrodermal activity appear during emotion.
- Interindividual variability of these cross-correlations are observed.
- One cluster of stress vulnerability with cross-correlations independent of emotion.
- Cross-correlations of the stress vulnerability cluster are dependent of anxiety trait.
- Cluster membership prediction by a machine learning model.

Abstract

The fast reaction of the autonomic nervous system (ANS) to an emotional challenge (EC) is the result of a functional coupling between parasympathetic (PNS) and sympathetic (SNS) branches. This coupling can be characterized by measures of cross-correlations between electrodermal activity (EDA) (under the influence of the SNS) and the RR interval (the interval between R peaks) (under the influence of the PNS and the SNS). Significant interindividual variability has previously been reported in SNS-PNS coupling in emotional situations, and the present study aimed to identify interindividual cross-correlation variability in ANS reactivity. We therefore studied EDA and the RR interval in 62 healthy subjects, recorded during a 24-minute EC. A Gaussian Mixture Model was used to cluster tonic EDA-RR cross-correlations during the EC. This identified two clusters that were characterized by significant or non-significant cross-correlations (SCC and NCC clusters, respectively). The SCC cluster reported higher negative emotion after the EC, while the NCC cluster reported higher scores on the Center for Epidemiologic Studies–Depression scale. The latter finding suggests that NCC is a pathological mood pattern with altered negative perception. Furthermore, a machine learning model that included three parameters indexing the functionality of both branches of the ANS, measured at baseline, predicted cluster membership. Our results are a first step in detecting dysfunctional ANS reactivity in general population.

Keywords

Emotion, cross-correlation, interindividual variability, nonlinear, autonomic nervous system, machine learning

1. Introduction

Emotional reactivity can be defined as the response of the autonomic nervous system (ANS) to an emotional stimulus. Typically, there is a joint reaction that involves both parasympathetic and sympathetic systems (McCraty et al., 1995). Electrodermal activity (EDA) and heart rate (HR) are physiological indices of ANS activity: EDA is under the influence of the cholinergic sympathetic system, and HR is under the influence of both sympathetic and parasympathetic systems (Kreibig, 2010). These two branches of the ANS interact closely, and the activity of one modulates the activity of the other (Thayer & Lane, 2009).

Examining moment-to-moment ANS responses during an emotional experience remains a methodological challenge (Golland et al., 2014; Kettunen & Keltikangas-Jarvinen, 2001). Since emotion is defined as a phasic response, several theoretical models assume that multiple patterns of body responses succeed each other during an emotional event (Scherer, 2009). Under this assumption, dynamic rather than steady point measurements are more informative. Findings from earlier studies support the idea that cross-correlation analysis can provide relevant indices of ANS activity, by comparing the dynamics of activities in both branches during an emotional experience (Golland et al., 2014).

Cross-correlations between EDA and HR have been used as a simplified index of ANS functioning in the past (Janig & Habler, 2000). This approach reduces the number of dimensions to be considered, and enables a continuous assessment of the balance between the two branches (Golland et al., 2014). Such an analysis is in line with the interest of nonlinear variables for each ANS signal. As there are several levels of regulation (Thayer & Lane, 2009), ANS oscillation is nonlinear (Basar & Guntekin, 2007) and can be described by appropriate indices (Reiter et al., 2020). These nonlinear variables provide an overview of the equilibrium of the system, describe its functioning and, more particularly, its flexibility (Young & Benton, 2015).

ANS regulation can be estimated by the Lyapunov exponent (LE), which is correlated to the size of the active biological neuronal pathway (Lajoie et al., 2014). The LE is a numeric value that characterizes the ability of a signal to be influenced (Pilant, 2020). An increase in the size of the active neuronal network leads to it being more influenced and, therefore, the LE increases (Lajoie et al., 2014). The LE is usually correlated with the Hurst exponent (HE) (Tarnopolski, 2016), which characterizes the ability of a signal to persist in the long term. This long-term memory appears to be a consequence of stability in the connectivity of an active neural network (Taylor et al., 2012).

SD1 and SD2 Poincaré indices reflect, respectively, short- and long-term signal variability, and provide information about the type of neural activity. When applied to the R-peak (RR) interval, short-term variability is known to be a marker of the effects of parasympathetic activity on the sinus node, since vagal effects are known to be faster than sympathetic ones (Hoshi et al., 2013; Mourot et al., 2004). SD2 is influenced by both tones (De Vito et al., 2002; Hoshi et al., 2013). In the case of heart rate variability (HRV), the SD1/SD2 ratio, which represents the relationship between the two components has been shown to be correlated to the HE (Hoshi et al., 2013). Nonlinear indices can, thus, indicate the dynamic functioning of the ANS (Reiter et al., 2020) and give a precise evaluation of system flexibility, in terms of variability, memory or control under stress (Young & Benton, 2015).

Although dynamic approaches have been shown to be useful in reducing variability in ANS responses to emotion, interindividual variability remains significant, and appears to be a function of numerous historical, environmental, and biological factors (Andrew et al., 2017; Boissy, 1995; Fan et al., 2014; Golland et al., 2014; Hot et al., 2005; Huang et al., 2018; von Holzen et al., 2016). Furthermore, anxiety, mood, and alexithymia have been found to be associated with a lack of ANS flexibility (Agorastos et al., 2020; Hoehn-Saric & McLeod, 2000; Koschke et al., 2009; Lischke et al., 2018; Udupa et al., 2007). While overall, these differences have been described for each branch of the ANS (Charkoudian & Wallin, 2014; Kirstein & Insel, 2004; Muhtadie et al., 2015), to the best of our knowledge interindividual differences in dynamic interactions between the two branches of the ANS have not been explored. More

specifically, questions remain not only about the functioning of each individual ANS branch, but also the dynamics of their interaction.

Hence, this exploratory study assesses the relevance and sensitivity of the combination of two methodological approaches: *i*) a cross-correlation analysis between the two branches of the ANS; and *ii*) the use of machine learning to identify profiles (clusters) of ANS reactivity. The first step was to identify the dynamic co-evolution of sympathetic and parasympathetic branches of the ANS during an emotional challenge (EC), and pinpoint clusters of inter-individual variability based on cross-correlations between EDA and RR intervals, measured as the tonic (e.g., skin conductance level) component of EDA.

Tonic and phasic components of EDA are underpinned by different neuroanatomical pathways and, therefore, different processes (Nagai et al., 2004; Ozawa et al., 2019). The tonic component covaries with ventromedial prefrontal and orbitofrontal cortex activities, while the phasic component is a function of activity in various regions of the brain, such as the hypothalamus, thalamus, striate and extrastriate cortices, anterior cingulate and insular cortices, and several lateral regions of the prefrontal cortex (Nagai et al., 2004; Ozawa et al., 2019). As a consequence, it is influenced by multiple inputs depending on the task, while the tonic component appears to be under the influence of attentional processes that are particularly enhanced in an emotional context (Nagai et al., 2004; Ozawa et al., 2019). These differences should make it possible to describe the ANS time course during an EC by capturing the degree of cross-correlation as a marker of autonomic adjustment. Thus, as a first step, the combination of variation in tonic EDA and RR outputs during an EC may provide a fine-grained assessment of individual emotional reactivity. Variability was characterized using physiological, sociodemographic, and psychological variables.

The second step in our work used a machine learning analysis to assess resting state ANS indices that best-predict emotional reactivity patterns. This is a major challenge, as cross-correlations are not observed beyond the context of emotional events (Golland et al., 2014). We used a Support Vector Machine (SVM)

learning method as it can combine several parameters, improving prediction capacity. This technique is particularly useful in a context where there are at least two factors (such as the two branches of the ANS).

2. Materials and methods

Results presented in this article were collected from two successive studies. The first validated the EC (Study I), and the second analyzed the dynamic cross-correlation between the two branches of the ANS during the same EC (Study II).

2.1. Subjects

Study I was conducted with 58 participants (72.5% women; mean age = 20.84±0.49 (standard error of the mean [SEM])), and Study II with 66 participants (88.71% women; mean age = 20.52±0.55). No significant differences were found for sociodemographic parameters between the two groups (Supplementary Table 1). Both studies were approved by the Ethics Committee of Savoie Mont Blanc University, France (CEREUS_2017_13). Written informed consent was obtained from each participant. Participants were recruited from among psychology students at Savoie Mont Blanc University and Grenoble Alpes University.

2.2. Procedure

Procedure common to both studies

Each participant was tested individually in an experimental room. Physiological sensors for the electrocardiogram (ECG) and EDA were attached. Recording was continuous throughout the experiment. To obtain a baseline measurement, participants were asked to rest without moving, and let their mind wander with their eyes open for 10 minutes. This period was chosen in order to have enough time to calculate ANS signal parameters. Emotional state was assessed using the Affective Slider (AS) (Betella & Verschure, 2016). The AS assessment was performed before and after the 10-minute baseline phase

(Figure 1). Then, participants watched a 24-minute video based on extracts from the movie *The Conjuring* (Wan, 2013). This duration was chosen to ensure immersion. At the end of the video, the AS assessment was repeated. This was followed by a 15-minute recovery period, and another AS assessment. This period was chosen in order to have enough time to calculate ANS signal parameters and to observe a recovery of physiological parameters. Finally, participants were asked to report the degree to which the video they had just watched was unpleasant and scary, using two analogue scales ranging from −50 (not unpleasant/scary at all) to +50 (very unpleasant/scary), with 0 corresponding to a neutral state.

Differences between studies

While watching the video, participants in Study I used a potentiometer to continuously evaluate their instantaneous emotional state. This real-time assessment validated the intensity of the experience. Because it was possible that this conscious activity would influence ANS reactivity (Park & Thayer, 2014; Park et al., 2013), the same assessment was not performed during Study II, in which we aimed to assess dynamic ANS change.

Power analysis

The necessary number of subjects was calculated using BiostaTGV ("BiostaTGV,"), based on a similar previous study (Golland et al., 2014). The earlier study recruited 27 subjects with the aim of observing significant cross-correlations. It found a correlation coefficient of around 0.6 during an emotional event, and standard deviation of around 0.1. In the present study, our goal was to observe at least two clusters, with a minimum difference of 15% and power of 90%, at a significance level of 0.05. The minimum number of subjects was identified as 52. This was increased by 10% for Study I (to compensate for technical problems in the emotional assessment system), and by 20% for Study II (to compensate for both technical problems and signal anomalies).

Study I: Validation of the emotional paradigm

A total of 58 participants were recruited. Of these, 37 provided an instantaneous emotional assessment of the movie and complete sociodemographic information; three provided an instantaneous emotional assessment and incomplete sociodemographic information (age, weight, and height were not recorded); and 18 only provided emotional assessment data.

Study II: The dynamic ANS model and the machine learning model

Among the 66 participants who were initially recruited, data from one was excluded due to a technical problem during the experiment (significant signal loss) and three were excluded due to a physiological anomaly (arrhythmia).

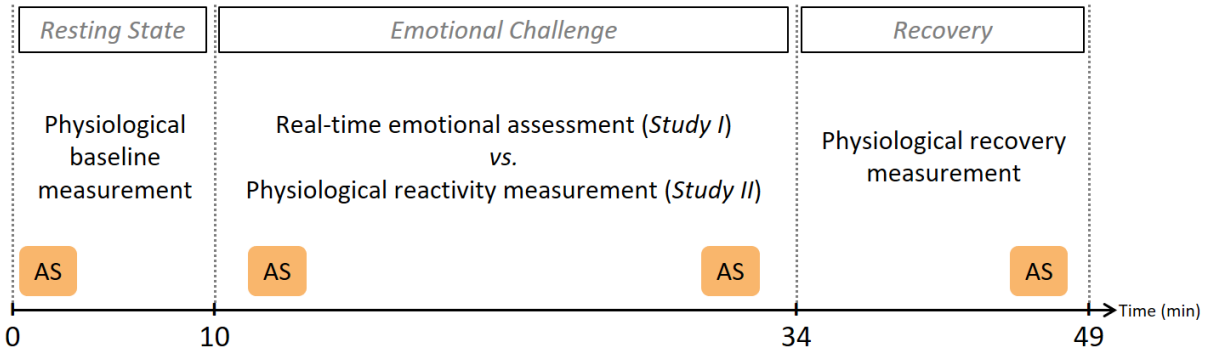

Figure 1: Experimental procedure for both studies. AS: Affective Slider assessment.

2.3.Sociodemographic data

Sociodemographic variables included age, weight, height, tobacco use, consumption of caffeine and psychotropic substances, medical treatments, sleep habits and sports practice.

2.4.Psychological assessment

The psychological assessment was based on a set of standardized instruments that included the following three questionnaires:

i. The Spielberger Trait Anxiety Inventory (STAI): a 20-item assessment in which higher scores indicate more trait anxiety (Spielberger, 1983).

ii. The Toronto Alexithymia Scale (TAS): a 20-item assessment in which higher scores indicate greater alexithymia (Loas et al., 1995). Three dimensions were evaluated: difficulty in identifying feelings, difficulty in describing feelings, and thoughts oriented toward external reality.

iii. The Center for Epidemiologic Studies–Depression (CES-D) scale: a 20-item assessment in which higher scores indicate a higher level of depressive symptoms (Fuhrer & Rouillon, 1989).

2.5. Affective Slider assessment

Participants' instantaneous emotional state was evaluated with the AS (Betella & Verschure, 2016). This assessment consists of two analogue scales, one addressing emotional valence, the other Arousal. In both cases, scales range from −50 (very negative) to +50 (very positive), with 0 corresponding to a neutral state. This measure was recorded between tasks (Figure 1).

2.6. Real-time emotional assessment

A real-time emotional assessment was carried out while participants watched the video in Study I. Subjects continuously moved a linear home-made potentiometer. Values ranged from 0 (minimal intensity) to 40 (maximal intensity). The sampling frequency was 2 Hz. A higher sampling frequency would have been possible, but would not have been relevant, given that we were seeking to measure a conscious, explicit behavioral response. The response was then normalized for each subject as a percentage of maximum intensity.

2.7. Physiological measures

The ECG was recorded with sensors placed on the chest, according to the DII standard Einthoven derivation. EDA was recorded by placing electrodes on the last phalanx of the index and middle fingers of the non-dominant hand. The signal was acquired by ECG 100 and GSR 100 amplifier modules connected

to a BioPac MP150 (BioPac Systems, Inc., CEROM, Paris, France). Acquisitions were performed with AcqKnowledge 4.1 software at a sampling frequency of 1000 Hz. ECG and EDA signals were recorded during the entire experiment and then transferred to MATLAB software (Mathworks, r2018a, Natick, Massachusetts, USA) for tonic and phasic EDA and RR post-acquisition processing.

2.8. Physiological signal preprocessing

R peaks were first detected automatically by an algorithm based on wavelet detection, and then comprehensively manually checked. In one case, peaks could not be manually identified, and the recording was considered artifacted and excluded. The EDA signal was first separated into phasic and tonic components by a validated algorithm (Greco et al., 2016), before being down-sampled from 1000 Hz to 2 Hz to allow it to be aligned with the interpolated inter-beat interval (IBI). Finally, it was smoothed by a moving median algorithm with a 10-point moving window, as previously reported (Golland et al., 2014). Both components of the time series were then detrended and normalized as *z*-scores, as recommended for cross-correlation analysis (Box et al., 2016; Golland et al., 2014).

2.9. Physiological signal analysis

2.9.1. IBI time series

2.9.1.1. Temporal analysis of RR intervals

The following temporal components of HRV were calculated from RR intervals: mean RR (the mean of RR intervals in ms); SDNN (the standard deviation of normal-to-normal RR intervals in ms); RMSSD (the root mean square of successive differences in ms); and HRV-TI (the Heart Rate Variability Triangular Index).

2.9.1.2. Frequency analysis of IBI time series

RR intervals were interpolated to a 2 Hz IBI time series that was then detrended. A fast Fourier transform using the Welch method with a moving window and an overlap of 50% was used to calculate spectral components of HRV parametric analyses: Very Low Frequencies (VLF): 0.002–0.04 Hz; Low Frequencies (LF): 0.04–0.15 Hz; and High Frequencies (HF): 0.15–0.5 Hz. VLF, LF and HF were calculated as a percentage of the sum of VLF+LF+HF.

2.9.2. HF time series

The 2 Hz detrended IBI time series was analyzed using a continuous wavelet transform. Following the method reported in the literature, a Morse wavelet with symmetry parameter equal to three, and time-bandwidth product equal to 60 were used. HF power was extracted as a percentage of the sum of VLF+LF+HF, after exclusion of the cone of influence. The previously-described nonlinear algorithms were applied, and Poincaré indices, the HE, and the largest LE were calculated as described earlier. These nonlinear indexes of HF time series have previously been described (Hoshi et al., 2013; Yeragani et al., 2002).

2.9.2.1. Nonlinear analysis of HF time series

Poincaré indices SD1 and SD2, the HE, and the LE of the HF time series were calculated.

Poincaré indices

Nonlinear Poincaré indices SD1 and SD2 describe the variability of the Poincaré plot, and were calculated from RR intervals. SD1 and SD2 provide an estimate of the dispersion of points perpendicularly, and along the line of identity, respectively. They therefore represent short- and long-term variability in the analyzed signals, respectively.

The Hurst exponent

The HE evaluates the long-term memory of a process (Tarnopolski, 2018). Its interpretation is a function of its value. A value above ½ suggests a persistent process that has long-term memory and a value below ½ suggests a non-persistent process with a short-term memory (Tarnopolski, 2016). The HE was calculated using a detrended moving mean algorithm, which was chosen because of its simple, closed-form processing (Tarnopolski, 2018).

The largest Lyapunov exponent

The largest LE (λ) indicates the exponential divergence/ convergence of an initially-considered point in a dynamic system in its phase space, within a time limit of infinity (i.e., the degree of sensitivity to initial conditions) (Tarnopolski, 2018). Considering two points close to the phase plane at times t=0 and t=t, and the distances between these points in the i^{th} direction, the LE is estimated as follows:

$$\lambda_i = \lim_{t\to\infty} \frac{1}{t} \log_2 \frac{|\delta x_i(0)|}{|\delta x_i(t)|}$$

where $\|\delta x_i(0)\|$ and $\|\delta x_i(t)\|$ are the Euclidean distances between the two points in the i^{th} direction at times t=0 and t, respectively (Pilant, 2020; Tarnopolski, 2018). The limit $t\to\infty$ is replaced by t that is sufficiently large, leading to the finite time LE (Pilant, 2020; Roth, 2009).

LE values above 0 are associated with chaos, and correspond to a deviation that grows exponentially as the number of iterations increases. Values equal to 0 are associated with a periodic or quasiperiodic signal, and indicate that deviation from the orbit remains steady regardless of the number of iterations (Dämmig & Mitschke, 1993). Among the numerous algorithms used to estimate LE, we selected Pilant's algorithm because of its simplicity and the closed form processing (Pilant, 2020). Non-MATLAB users can download and read the algorithm using a standard text editor.

2.9.3. EDA time series

Poincaré indices, the HE, and the LE were calculated as described earlier for tonic EDA time series.

2.10. Correlation analysis

Sampling frequencies for the two signals were aligned. The 2 Hz detrended IBI time series was filtered below 0.04 Hz in order to remove low components insufficiently present in 60 s window. The last time series were then normalized as *z*-scores. A cross-correlation analysis between the IBI time series and the tonic EDA time series was performed for each subject using moving windows according to Golland et al. (Golland et al., 2014). Briefly, the analysis is based on short (t=60 s) overlapping (Δt=30 s) time segments. For each segment, and for each individual the maximum correlation (within ± 5-s lags) was identified between the two series. In each case, a nonparametric bootstrapping procedure with surrogate data allowed us to control the statistical significance of the result. Surrogate data were obtained by randomizing segments in the time series. This procedure was repeated 1000 times. As described in previous work (Golland et al., 2014), the statistical likelihood of a cross-correlation in each time window was assessed nonparametrically using the Wilcoxon rank sum test against synthetic control data. Obtained *p*-values were corrected for multiple comparisons using the false discovery rate (FDR) procedure (Benjamini & Hochberg, 1995).

2.11. Clustering

2.11.1. Evaluation of the optimal number of clusters

Clusters of subjects with the same emotional response were identified from cross-correlations between the RR interval and the tonic EDA signal observed during the eight, intensely emotional 60 s windows of the movie (4–5, 6–7, 8–9, 10–11, 12–13, 17–18, 19–20, and 21–22 min). Values were calculated for each individual. The clustering of subjects was performed on these last 8 variables by using the Calinski–Harabasz algorithm for Gaussian model mixture distribution as available in MATLAB software. The

Calinski–Harabasz non-supervised cluster solution algorithm was chosen as it uses clustering criteria based on the ratio of variances to provide a robust heuristic index (Andrade et al., 2020). Thus, a well-defined cluster has a large between-cluster variance and a small within-cluster variance. The optimal number of clusters is chosen according to a criterion based on these parameters. One to six cluster solutions were tested. The maximum number of iterations to reach convergence was set at 1000, and a diagonal covariance matrix was used. Solutions with the best fit were considered optimal. This solution without *a priori* has retrieved an optimal number of 2 clusters.

2.11.2. Cluster membership

Membership of one of the two clusters was determined from the eight cross-correlation values that determined the dynamics of each individual's responses using a Gaussian Mixture Model. This method was selected to study interindividual variability as, by definition, the latter follows a Gaussian distribution. MATLAB's *cluster* algorithm was used, with the maximum number of iterations to reach convergence set at 1000. Here again, a diagonal covariance matrix was used. The Gaussian model assigns query data points to the multivariate normal components that maximize the component posterior probability, given the data. The method established the following cluster membership: cluster 1 (n=30) and cluster 2 (n=32).

2.12. Machine learning

The ability of baseline parameters to predict the distribution of subjects within clusters was trained and cross-validated using a linear kernel SVM model. The linear kernel is widely used due to its robustness. To further increase robustness, a classical cross-validated model was used. First, data were randomly partitioned into 10 sets. Then, for each set, the algorithm reserved the set as validation data, and trained the model on the other nine sets. The out-of-sample misclassification rate was used to assess performance.

2.13. Statistical analysis

Statistical analyses were performed with MATLAB, Cohen's effect sizes were calculated with G*Power. One-way factorial analyses of variance (ANOVAs) were performed to compare means of the two clusters. As the duration of baseline, EC, and recovery phases were different, repeated measures ANOVAs could not be used to compare HRV results because most parameters are a function of the sample size. Other, time-insensitive parameters were analyzed with repeated measures ANOVAs for Time and Group main effects, and their interaction. Time effects identified changes in measures between baseline, EC, and recovery. Group effects identified differences between clusters 1 and 2. Group×Time effects reflect the combined effects of Time and Group. When the ANOVA revealed a significant effect, partial eta squared and Cohen's f effect size were calculated to estimate its size. According to the work of Schäfer and Schwarz applied to psychology domain, we considerated that an effect size of 0.2 as small, higher than 0.4 as medium and higher than 0.6 as large (Schafer & Schwarz, 2019). Partial eta squared of 0.01 indicates a small effect, of 0.06 a medium effect and 0.14 a large effect. Clusters were characterized by the mean value of the cross-correlation during each window. This was linked to other psychological data using Pearson correlations for each cluster.

For categorical variables, Chi-Square independence tests were used. When significant, a Cohen's w effect size was calculated. According to basic rules for Cohen's w, a w of 0.10 indicates a small effect, of 0.30 a medium effect and 0.50 a large effect (Cohen, 1988).

The predictive power of each variable was assessed with receiver operating characteristic (ROC) curves. The cut-off was associated with an area under the curve (AUC) above 0.8. Significance was set at $p<0.05$. As for cross-correlation, *p*-values were corrected for multiple comparisons using the FDR procedure (Benjamini & Hochberg, 1995). Data are presented as mean ± SEM.

3. Results

3.1. Study I: Validation of the EC

As they watched the video, subjects evaluated real-time emotional intensity (Figure 2). Our result highlighted a progressive increase in global intensity as a function of time, along with a few bursts. As cross-correlations between EDA and the RR interval have previously only been observed during emotional bursts (Golland et al., 2014; Hsieh et al., 2011), this result confirmed that the EC was an efficient way to study cross-correlations between the two branches of the ANS.

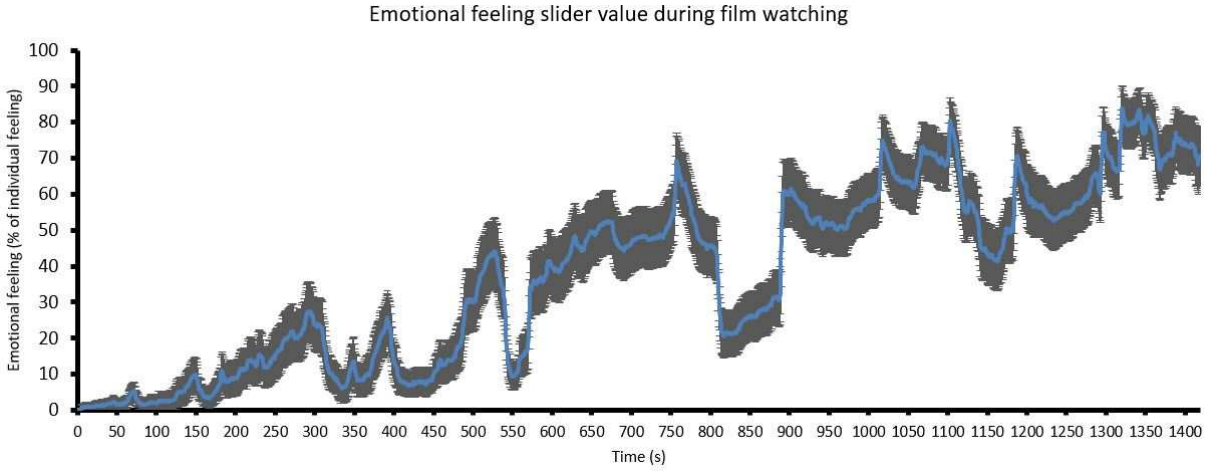

Figure 2: Emotional intensity as a function of time. Emotional intensity was expressed as a percentage of individual feeling measured using a potentiometer (see Materials and Methods). The blue line represents the mean for all subjects. Black bars represent the 95% confidence interval.

3.2. Study II: Evaluation of the autonomic dynamic during the EC

3.2.1. Physiological identification of emotional bursts during the EC

In order to align the self-reported emotion scores obtained in Study I (Figure 2) with cross-correlation results, we calculated mean self-reported emotion intensity for each 60 s window (Figure 3.A). This identified eight windows with peak emotional intensity (4–5, 6–7, 8–9, 10–11, 12–13, 17–18, 19–20, and

21–22 min; Figure 3.A). Significant negative cross-correlations between the RR interval and tonic EDA (i.e., low RR and high EDA) were only observed in two windows: 12–13 min (r=−0.36 ± 0.05, p <0.05); and 12 min 30 s to 13 min 30 s (r=−0.35 ± 0.06, p <0.05; Figure 3.B).

As our earlier work had identified that significant cross-correlations are only observed during emotional events (Golland et al., 2014), we limited the search for interindividual variability in cross-correlations between the RR interval and tonic EDA to these eight bursts. An automated analysis of the optimal number of clusters for these eight cross-correlations identified two: cluster 1 (n=30); and cluster 2 (n=32). Significant cross-correlations were found among individuals in cluster 1 during the EC, but not cluster 2 (Figure 3.C). Therefore, cluster 1 was labelled the "significant correlation cluster" (SCC), and cluster 2 the "non-significant correlation cluster" (NCC). Finally, no significant cross-correlation was observed for either cluster at baseline or recovery (Supplemental Figures 1A to D).

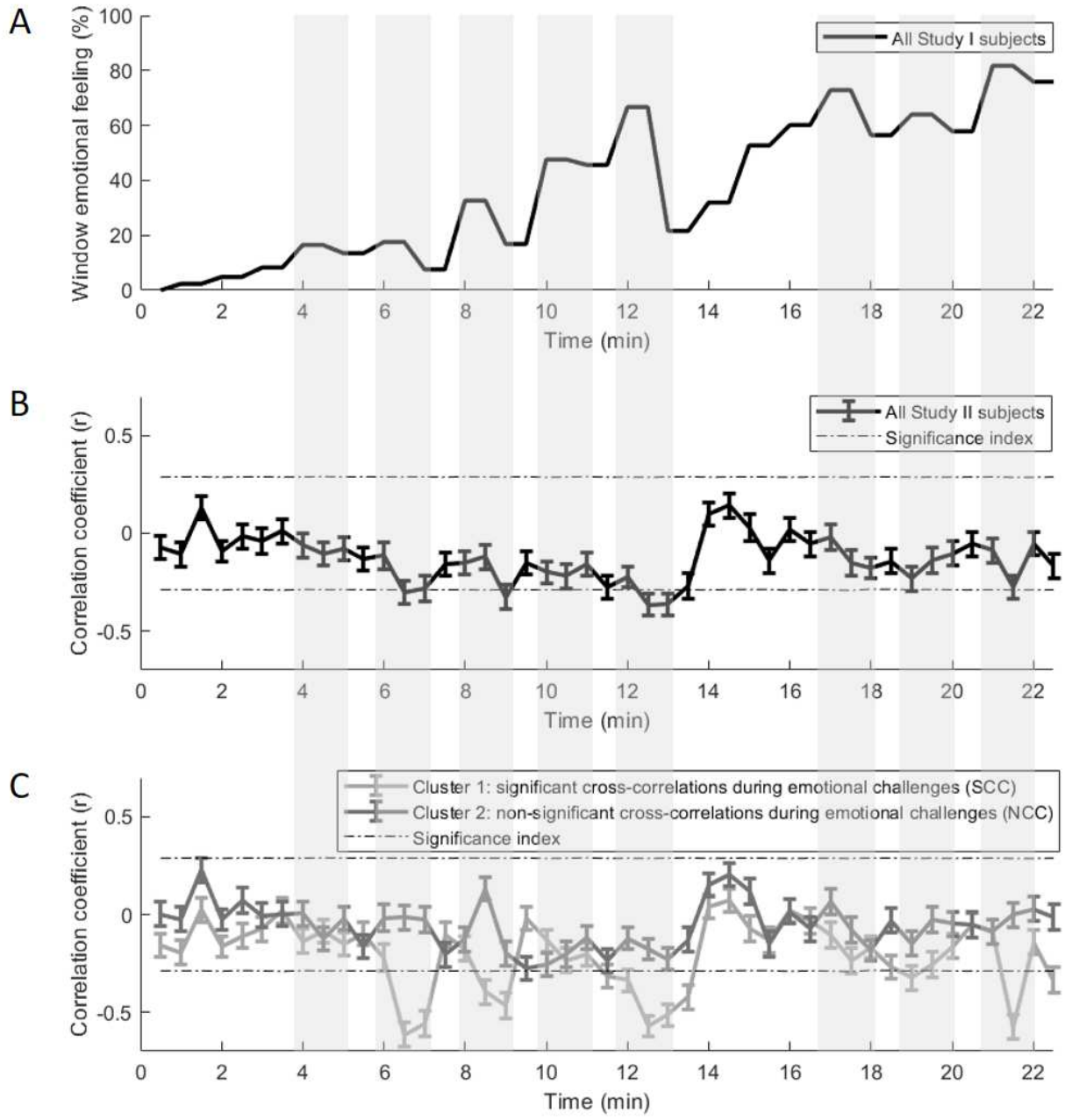

Figure 3: Cross-correlations between tonic EDA and the RR interval during the EC.

A, B, C: Vertical gray zones represent the eight emotional peaks during the EC. Results are expressed as mean ± SEM. Dotted horizontal lines represent FDR-corrected upper and lower limits of significance

(q<0.05). **A**: Mean emotional intensity as a percentage for overlapping windows (Study I). **B**: Cross-correlation coefficients (r) for overlapped windows (window size = 60 s, with an overlap of 50% between two windows) for all subjects in Study II. **C**: Cross-correlation coefficients (r) for overlapped windows (window size = 60 s, with an overlap of 50% between two windows) for each cluster (Study II).

3.2.2. Physiological characterization of clusters

No difference was observed between clusters at baseline or recovery. However, Table 1 shows that during the EC the SCC group was characterized by a less chaotic distribution (LE) of tonic EDA (F(1,60)=9.5, FDR-corrected p<0.05, observed power=0.86, partial eta-squared=0.14, Cohen's f=0.53). Results for all tested physiological variables are reported in Supplementary Table 2.

Table 1: Physiological results as a function of cluster and measurement time. Results are expressed as mean (± SEM). As the three measurement periods (baseline, EC, and recovery) are not of the same duration, a repeated measures ANOVA cannot be used. Only significant results after FDR correction (q<0.05) for the one-way ANOVA for each period are shown.

	Baseline				EC				Recovery			
	Significant correlation cluster (SCC)	Non-significant correlation cluster (NCC)	p-Value corrected by FDR of 1-way ANOVA	Observed power	Significant correlation cluster (SCC)	Non-significant correlation cluster (NCC)	p-Value corrected by FDR of 1-way ANOVA	Observed power	Significant correlation cluster (SCC)	Non-significant correlation cluster (NCC)	p-Value corrected by FDR of 1-way ANOVA	Observed power
EDA signal												
LE tonic EDA	1.34 (± 0.07)	1.28 (± 0.07)	F(1,60)=0.32; p=0.80	0.09	**1.78 (± 0.04)**	**1.51 (± 0.08)**	**F(1,60)=9.5; p=0.045 partial eta-squared=0.14 Cohen's f=0.53**	**0.86**	1.41 (± 0.05)	1.33 (± 0.07)	F(1,60)=0.77; p=0.71	0.14

3.2.3. Psychological characterization of clusters

Psychological characterization consisted of reported emotional intensity at different times of the procedure, and an initial psychopathological self-report questionnaire. Table 2 shows AS scores, and highlights that the NCC group perceived the EC less negatively than the SCC group (F(1,60) = 11.50, FDR-corrected p<0.01, observed power=0.92, partial eta-squared=0.16, Cohen's f=0.63).

Table 2: Reported AS as a function of cluster. *p*-values are calculated with repeated measure ANOVAs of Valence and Arousal, and a one-way ANOVA with FDR correction (q<0.05) for the overall evaluation of emotion. Results are expressed as mean (± SEM).

		Significant correlation cluster (SCC)	Non-significant correlation cluster (NCC)	Statistics
Valence	Before baseline	19.40 (± 2.16)	18.44 (± 2.97)	Repeated ANOVA: interaction F(3,180)=0.91; p=0.44; observed power=0.25 group effect F(1,60)=1.35; p=0.25; observed power=0.21
	After baseline	12.53 (± 2.37)	17.84 (± 2.60)	
	After video	-4.7 (± 3.66)	0.75 (± 3.31)	
	After recovery	5.63 (± 1.98)	9 (± 2.63)	
Arousal	Before baseline	-6.87 (± 2.93)	0.88 (± 3.31)	Repeated ANOVA: interaction F(3,180)=1.61; p=0.19; observed power=0.42 group effect F(1,60)=0.01; p=0.93; observed power=0.05
	After baseline	-20.83 (± 3.25)	-20.91 (± 3.68)	
	After video	18.97 (± 3.11)	13.97 (± 3.75)	
	After recovery	-9.37(± 3.48)	-13.13 (± 4.75)	
Final evaluation	Unpleasant video feeling	10.43 (± 4.18)	4.53 (± 3.94)	1-way ANOVA: F(1,60)=1.06; p corrected=0.31; observed power=0.17
	Scary video feeling	18.7 (± 2.98)	9.47 (± 3.78)	1-way ANOVA: F(1,60)=3.62; p corrected=0.09; observed power=0.46
	Negative video feeling	**15.8 (± 3.23)**	**-3.06 (± 4.46)**	**1-way ANOVA: F(1,60)=11.50; p corrected=0.003; observed power=0.92 partial eta-squared=0.16; Cohen's f=0.63**

Table 3 highlights that the NCC group scored higher on the CES-D scale than the SCC group, indicating more depressive symptoms.

Table 3: Psychological indicators as a function of cluster. *p*-values were calculated using a one-way ANOVA. Results are expressed as mean (±SEM).

	Significant correlation cluster (SCC)	Non-significant correlation cluster (NCC)	Statistics
STAI-Trait	44.87 (±1.86)	49.17 (±1.75)	1-way ANOVA: F(1,60)=2.82; p corrected=0.25; observed power=0.38
CES-D	**15.7 (±1.73)**	**22.72 (±2.1)**	**1-way ANOVA: F(1,60)=6.53; p corrected=0.05; observed power=0.71; partial eta-squared=0.10; Cohen's f=0.41**
TAS-20: difficulties in identifying feelings	16.37 (±1.05)	18.28 (±1.27)	1-way ANOVA: F(1,60)=1.33; p corrected=0.31; observed power=0.21
TAS-20: difficulties in describing feelings	13.47 (±0.93)	13.94 (±0.93)	1-way ANOVA: F(1,60)=0.13; p corrected=0.72; observed power=0.06
TAS-20: thoughts oriented toward external reality	16.8 (±0.76)	15.47 (±0.66)	1-way ANOVA: F(1,60)=1.76; p corrected=0.31; observed power=0.25

3.2.4. Health behavior in clusters

While no difference was found between the two clusters with respect to sociodemographic characteristics, health behaviors did differ (Table 4). Specifically, those in the NCC cluster were more likely to smoke than those in the SCC cluster.

Table 4: Demographics and health behavior as a function of cluster. *p*-values were calculated using a one-way ANOVA or χ^2 test. Results are expressed as mean (± SEM).

	Significant correlation cluster (SCC)	Non-significant correlation cluster (NCC)	Statistics
Age (year)	20.73 (±1.08)	20.34 (±0.51)	1-way ANOVA: F(1,60)=0.11; p corrected =0.97; observed power=0.06
Height (cm)	166.37 (±1.13)	166.38 (±1.35)	1-way ANOVA: F(1,60)=0.00; p corrected =1; observed power=0.05
Weight (kg)	62.57(±2.32)	63.06 (±3.41)	1-way ANOVA: F(1,60)=0.01; p corrected =0.98; observed power=0.05
Gender	3 men / 27 women (10%)	4 men / 28 women (12.5%)	χ^2 p corrected =0.97; power (1-β)=0.06
Smoking	**2 yes / 28 no (6.7%)**	**13 yes / 19 no (40.6%)**	**χ^2 p corrected =0.03; power (1-β)=0.88; Cohen's w=0.55**
Coffee or energy drink use	8 yes/ 22 no (26.7%)	14 yes / 17 no (45.2%)	χ^2 p corrected =0.46; power (1-β)=0.32
Drug use	6 yes / 24 no (20%)	8 yes / 24 no (25%)	χ^2 p corrected =0.97; power (1-β)=0.08
Regular sports	20 yes / 10 no (66.7%)	17 yes / 15 no (53.1%)	χ^2 p corrected =0.56; power (1-β)=0.19
Slept well the previous night	21 yes / 9 no (70%)	25 yes / 5 no (83.3%)	χ^2 p corrected =0.51; power (1-β)=0.23
Bedtime	11:55 p.m. (±19 min)	11:49 p.m. (±30 min)	1-way ANOVA: F(1,60)=0.02; p corrected =0.98; observed power=0.05
Waking hour	7:03 a.m. (±12 min)	7:49 a.m. (±19 min)	1-way ANOVA: F(1,60)=4.11; p corrected =0.22; observed power=0.51
Sleep duration (seconds)	25738 (±1575.2)	28800 (±1671.6)	1-way ANOVA: F(1,60)=1.77; p corrected =0.51; observed power=0.26
Sleepy today	12 yes / 18 no (40%)	15 yes / 17 no (46.9%)	χ^2 p corrected =0.97; power (1-β)=0.08
Concentration difficulties	5 yes / 25 no (16.7%)	15 yes / 17 no (46.9%)	χ^2 p corrected =0.07; power (1-β)=0.72

3.2.5. Functional patterns in clusters

To study each cluster individually, we summarized cross-correlation dynamics as the mean for each emotional burst for each participant (a cross-correlation reduction). This identified that (negative) cross-correlation values were higher among the SCC cluster (r=–0.37±0.03) than in the NCC group (r=–0.07±0.03; F (1,60)=69.89, p<0.001, partial eta-squared=0.54, observed power=1.00, Cohen's f=0.85). This variable can be used to study functional correlates in each cluster by testing Pearson correlations between it and psychological variables or subjective emotion. In the following, only significant results are reported.

In the NCC cluster, no correlation was found between mean cross-correlations during emotional bursts and subjective emotion or psychological variables. However, in the SCC cluster, they were correlated with subjective valence after video recording (r=0.43, corrected p<0.05), unpleasant emotions (r =–0.49, corrected p<0.01), and feeling scared (r=–0.45, corrected p<0.05). This finding indicates that the stronger

411 the negative cross-correlation between the RR interval and EDA while watching the movie, the greater
412 the perception of unpleasantness and feeling scared.

413 #### 3.2.6. Predicting clusters from baseline data with machine learning

414 First, ROC curves were used to evaluate the predictive power of each baseline variable individually. The
415 prediction of clusters using physiological variables or a single factor (identified by factor analysis)
416 yielded AUCs no higher than 0.63. These values are considered poor, as good predictive power is
417 associated with an AUC above 0.8. Then, a machine learning model was used to predict the distribution
418 of subjects within the two clusters using baseline physiological variables. The machine learning algorithm
419 automatically chose variables with the most predictive power. The search for new variables ended when
420 no additional variable increased the predictive power of the model (the list of variables is given in
421 Supplementary Table 2).

422 The cross-validated SVM model resulted in a prediction of 74.19% using only three baseline
423 physiological variables: the HE of tonic EDA; the percentage of HF; and the LE of HF. Two nonlinear
424 variables were automatically chosen by the model, suggesting that the nonlinear characteristics of both
425 EDA and HF signals are important baseline characteristics in predicting cross-correlation ANS
426 functioning during the EC. However, and interestingly, no difference between clusters was observed at
427 baseline for these variables when they were considered independently (Supplementary Table 2).

428 ## 4. Discussion

429 The goal of this study was to identify the dynamical coevolution of SNS and PNS during an EC and to
430 describe clusters interindividual variability based on dynamical cross-correlations between EDA and RR
431 intervals. Our study addresses two challenges. First, it is not possible to assess both moment-to-moment
432 emotional state, and the true emotional level when attention is focused on the emotional event (Park &

433 Thayer, 2014; Park et al., 2013). Second, the self-assessment of emotion can itself be considered as a
434 cognitive regulation task that may reduce intensity. Thus, we ran two studies, one to assess subjective
435 emotion (Study I), and the second to record objective emotion (Study II). Our results highlight cross-
436 correlations between tonic EDA and RR signals, and the existence of two profiles linking the two
437 branches of the ANS during an EC. The first is characterized by sympathetic activation coupled with
438 parasympathetic deactivation that marks the most emotionally-intense moments. The second is
439 characterized by a lack of functional coupling within the ANS, associated with low emotional feeling
440 during the EC and marked depressive symptomatology. Moreover, an exploratory machine learning
441 analysis allowed us to categorize and predict these two clusters based on ANS measurements taken at
442 rest.

443 Our study supports previous findings (Golland et al., 2014), which show that emotional arousal is
444 associated with cross-correlations between HR and EDA signals. In the present study, a decrease in the
445 RR interval duration was associated with a fast, transient disequilibrium between sympathetic and
446 parasympathetic systems that favored the sympathetic system during an EC. The cross-correlation
447 between these two variables underlies the functional coordination (or coupling) of the two branches of the
448 ANS.

449 **4.1. Interindividual variability in dynamic emotional reactions**

450 At the same time, our study goes further, and demonstrates the existence of two clusters of cross-
451 correlations using a data-driven approach. These interindividual differences have not been reported
452 previously, probably because individuals with no significant cross-correlations were excluded in earlier
453 studies, or were masked in a group analysis (Golland et al., 2014).

454 Specifically, the existence of two clusters suggests that there is a difference in ANS flexibility with
455 respect to the interplay between its two branches (Young & Benton, 2015). Interindividual variability
456 underlying variation in flexibility has already been identified using a clustering *p*-technique applied to

cardiovascular activity (Friedman & Santucci, 2003). The two autonomic branches of the ANS are mutually inhibiting and globally antagonistic (Burnstock, 2008), and this can occur at different levels of regulation, highlighting the global flexibility of brain function (Bornemann et al., 2019; Ondicova & Mravec, 2010; Young & Benton, 2015).

In the present study, the SCC cluster was characterized by greater chaos (higher LE) in tonic EDA compared to the NCC group, suggesting that the sympathetic nervous system has a more complex regulatory network (Lajoie et al., 2014) and is more sensitive to initial recording conditions. Hence, this higher degree of chaos is consistent with a higher level of regulation. As tonic EDA is under the influence of both the ventromedial prefrontal and orbitofrontal cortices, one or both could account for this finding. Medial orbitofrontal cortex activity, which is involved in subjective emotional experience, is lower in depressive patients, while activity in lateral orbitofrontal and ventromedial cortices is increased (Koenigs & Grafman, 2009; Rolls, 2019). These changes in the neural network could account for our observed changes in tonic EDA. Functional neuroimaging studies would supplement our initial cluster characterization and clarify the role of the cortices.

From a psychological point of view, those in the SCC cluster reported fewer depressive symptoms, suggesting good mental health. Furthermore, we observed an association between mean cross-correlations and emotional valence after the EC, notably with respect to unpleasant and scary variables, indicating congruency between the physiological reaction and emotional feeling as the movie was watched. These observations are in line with Thayer and Lane who reported that individuals with high resting HRV produce more context-appropriate emotional responses (Thayer & Lane, 2009). Furthermore, reduced HRV and flexibility have been associated with depression (Sgoifo et al., 2015).

In contrast, members of the NCC cluster reported higher levels of depressive symptoms (on the CES-D). Depressive symptoms difference between SCC and NCC was characterized by a medium effect size, nevertheless has to be considered since the mean level of NCC almost reached the threshold for

depression (Morin et al., 2011). This depressive dimension is consistent with their propensity to smoke (Fluharty et al., 2017), and a lack of autonomic flexibility reflected in an aberrant vagal response under challenge (Agorastos et al., 2020). Depressive symptoms have long been associated with undifferentiated negative emotions (Willroth et al., 2020). Overall, unlike the SCC cluster, we did not observe congruency between the autonomic dynamic and emotion.

4.2.Predicting emotional reactions

Predicting cluster membership on the basis of emotional regulation is not possible with a single variable. Classic one-dimension methods using ROC curves are insufficient. Thus, we used a machine learning technique to aggregate the pertinent dimensions. This revealed that three physiological baseline variables (including nonlinear dimensions of both EDA and HF time series) were able to predict up to 74% of high- and low-degree cross-correlation clustering and, therefore, the quality of emotional regulation under EC conditions. This prediction level is very close to the 80% threshold indicating good prediction ability. The fact that only three variables were used suggests good reproducibility. Moreover, these three variables appear to be important baseline predictors of the dynamics of parasympathetic activity (through the HF value), sympathetic persistence (through the HE of the tonic EDA), defined as the ability of the sympathetic system to maintain the same long-term kinetic, and parasympathetic determinism (through the LE of the HF), defined as the ability of the parasympathetic system to be exponentially disturbed.

While none of these baseline variables considered individually can identify the two clusters, their combination can. It should be noted that they reflect both sympathetic and parasympathetic markers, which is consistent with the idea of a co-dynamic ANS response to an EC.

4.3. Limitations

Our machine learning model is deliberately simplified to ensure its robustness and make it possible to draw conclusions. A better prediction level could be obtained with more a complex separation plan which

504 could be justified in context of the use of nonlinear variables. However, any generalization would require
505 a larger cohort to be valid. Second, this exploration of the characteristics of interindividual variability is a
506 pilot study and although promising, our results must be confirmed by further work. Another study of
507 interindividual variability based specifically on cardiovascular responsivity has identified a greater
508 number of clusters (four or five) in the context of three other laboratory stressors, suggesting that the
509 clustering solution might differ as a function of the stressor (Allen et al., 1991). Finally, our study is
510 limited by the fact that the majority of participants were young female students. It is possible that anxio-
511 depressive factors are more frequent in this group than in the general population (Dahlin et al., 2005).

512 ### 4.4. Conclusions

513 Despite the limitations noted above, our results are a promising step forward in the study of the
514 psychophysiological processes that are involved in various chronic pathologies that affect both mental
515 and somatic health.

516 ## 5. References

517 Agorastos, A., Stiedl, O., Heinig, A., Sommer, A., Hager, T., Freundlieb, N., Schruers, K. R.,
518 Demiralay, C., 2020. Inverse autonomic stress reactivity in depressed patients with and
519 without prior history of depression. J. Psychiatr. Res. 131, 114-118.
520 https://doi.org/10.1016/j.jpsychires.2020.09.016.
521 Allen, M. T., Boquet, A. J., Jr., Shelley, K. S., 1991. Cluster analyses of cardiovascular
522 responsivity to three laboratory stressors. Psychosom. Med. 53(3), 272-288.
523 https://doi.org/10.1097/00006842-199105000-00002.
524 Andrade, D., Takeda, A., Fukumizu, K., 2020. Robust Bayesian model selection for variable
525 clustering with the Gaussian graphical model. Statistics and Computing 30(2), 351-376.
526 https://doi.org/10.1007/s11222-019-09879-9.
527 Andrew, M. E., Violanti, J. M., Gu, J. K., Fekedulegn, D., Li, S., Hartley, T. A., Charles, L. E.,
528 Mnatsakanova, A., Miller, D. B., Burchfiel, C. M., 2017. Police work stressors and
529 cardiac vagal control. Am. J. Hum. Biol. 29(5). https://doi.org/10.1002/ajhb.22996.
530 Basar, E., Guntekin, B., 2007. A breakthrough in neuroscience needs a "Nebulous Cartesian
531 System" Oscillations, quantum dynamics and chaos in the brain and vegetative system.
532 Int. J. Psychophysiol. 64(1), 108-122. https://doi.org/10.1016/j.ijpsycho.2006.07.012.

Benjamini, Y., Hochberg, Y., 1995. Controlling the False Discovery Rate: A Practical and Powerful Approach to Multiple Testing Journal of the Royal Statistical Society. Series B: Methodological 57, 289-300. https://doi.org/10.2307/2346101.

Betella, A., Verschure, P. F., 2016. The Affective Slider: A Digital Self-Assessment Scale for the Measurement of Human Emotions. PLoS ONE 11(2), e0148037. https://doi.org/10.1371/journal.pone.0148037.

BiostaTGV. Retrieved from http://biostatgv.sentiweb.fr/

Boissy, A., 1995. Fear and fearfulness in animals. Q. Rev. Biol. 70(2), 165-191. https://doi.org/10.1086/418981.

Bornemann, B., Kovacs, P., Singer, T., 2019. Voluntary upregulation of heart rate variability through biofeedback is improved by mental contemplative training. Sci. Rep. 9(1), 7860. https://doi.org/10.1038/s41598-019-44201-7.

Box, G. E. P., Jenkins, G. M., Reinsel, G. C., Ljung, G. M., 2016. Time series analysis : forecasting and control (Fifth edition / ed.). John Wiley & Sons, Inc., Hoboken, New Jersey.

Burnstock, G., 2008. Unresolved issues and controversies in purinergic signalling. J. Physiol. 586(14), 3307-3312. https://doi.org/10.1113/jphysiol.2008.155903.

Charkoudian, N., Wallin, B. G., 2014. Sympathetic neural activity to the cardiovascular system: integrator of systemic physiology and interindividual characteristics. Compr. Physiol. 4(2), 825-850. https://doi.org/10.1002/cphy.c130038.

Cohen, J., 1988. Statistical Power Analysis for the Social Sciences (2nd ed.). Lawrence Erlbaum Associates, Hillsdale, New Jersey.

Dahlin, M., Joneborg, N., Runeson, B., 2005. Stress and depression among medical students: a cross-sectional study. Med. Educ. 39(6), 594-604. https://doi.org/10.1111/j.1365-2929.2005.02176.x.

Dämmig, M., Mitschke, F., 1993. Estimation of Lyapunov exponents from time series: the stochastic case. Physics Letters A 178(5), 385-394. https://doi.org/10.1016/0375-9601(93)90865-W.

De Vito, G., Galloway, S. D., Nimmo, M. A., Maas, P., McMurray, J. J., 2002. Effects of central sympathetic inhibition on heart rate variability during steady-state exercise in healthy humans. Clin. Physiol. Funct. Imaging 22(1), 32-38. https://doi.org/10.1046/j.1475-097x.2002.00395.x.

Fan, T., Fang, S. C., Cavallari, J. M., Barnett, I. J., Wang, Z., Su, L., Byun, H. M., Lin, X., Baccarelli, A. A., Christiani, D. C., 2014. Heart rate variability and DNA methylation levels are altered after short-term metal fume exposure among occupational welders: a repeated-measures panel study. BMC Public Health 14, 1279. https://doi.org/10.1186/1471-2458-14-1279.

Fluharty, M., Taylor, A. E., Grabski, M., Munafo, M. R., 2017. The Association of Cigarette Smoking With Depression and Anxiety: A Systematic Review. Nicotine Tob. Res. 19(1), 3-13. https://doi.org/10.1093/ntr/ntw140.

Friedman, B. H., Santucci, A. K., 2003. Idiodynamic profiles of cardiovascular activity: a P-technique approach. Integr. Physiol. Behav. Sci. 38(4), 295-315. https://doi.org/10.1007/BF02688859.

Fuhrer, F., Rouillon, F., 1989. The French version of the CES-D (Center for Epidemiologic Studies-Depression Scale)]. Psychiatrie & Psychobiologie 4(3), 163-166. https://doi.org/10.1017/S0767399X00001590.

Golland, Y., Keissar, K., Levit-Binnun, N., 2014. Studying the dynamics of autonomic activity during emotional experience. Psychophysiology 51(11), 1101-1111. https://doi.org/10.1111/psyp.12261.

Greco, A., Valenza, G., Lanata, A., Scilingo, E. P., Citi, L., 2016. cvxEDA: A Convex Optimization Approach to Electrodermal Activity Processing. IEEE Trans. Biomed. Eng. 63(4), 797-804. https://doi.org/10.1109/TBME.2015.2474131.

Hoehn-Saric, R., McLeod, D. R., 2000. Anxiety and arousal: physiological changes and their perception. J. Affect. Disord. 61(3), 217-224. https://doi.org/10.1016/s0165-0327(00)00339-6.

Hoshi, R. A., Pastre, C. M., Vanderlei, L. C., Godoy, M. F., 2013. Poincare plot indexes of heart rate variability: relationships with other nonlinear variables. Auton. Neurosci. 177(2), 271-274. https://doi.org/10.1016/j.autneu.2013.05.004.

Hot, P., Leconte, P., Sequeira, H., 2005. Diurnal autonomic variations and emotional reactivity. Biol. Psychol. 69(3), 261-270. https://doi.org/10.1016/j.biopsycho.2004.08.005.

Hsieh, F., Ferrer, E., Chen, S., Mauss, I. B., John, O., Gross, J. J., 2011. A Network Approach for Evaluating Coherence in Multivariate Systems: An Application to Psychophysiological Emotion Data. Psychometrika 76(1), 124-152. https://doi.org/10.1007/s11336-010-9194-0.

Huang, J. H., Chang, H. A., Fang, W. H., Ho, P. S., Liu, Y. P., Wan, F. J., Tzeng, N. S., Shyu, J. F., Chang, C. C., 2018. Serotonin receptor 1A promoter polymorphism, rs6295, modulates human anxiety levels via altering parasympathetic nervous activity. Acta Psychiatr. Scand. 137(3), 263-272. https://doi.org/10.1111/acps.12853.

Janig, W., Habler, H. J., 2000. Specificity in the organization of the autonomic nervous system: a basis for precise neural regulation of homeostatic and protective body functions. Prog. Brain Res. 122, 351-367. https://doi.org/10.1016/s0079-6123(08)62150-0.

Kettunen, J., Keltikangas-Jarvinen, L., 2001. Intraindividual analysis of instantaneous heart rate variability. Psychophysiology 38(4), 659-668. https://doi.org/10.1111/1469-8986.3840659.

Kirstein, S. L., Insel, P. A., 2004. Autonomic nervous system pharmacogenomics: a progress report. Pharmacol. Rev. 56(1), 31-52. https://doi.org/10.1124/pr.56.1.2.

Koenigs, M., Grafman, J., 2009. The functional neuroanatomy of depression: distinct roles for ventromedial and dorsolateral prefrontal cortex. Behav. Brain Res. 201(2), 239-243. https://doi.org/10.1016/j.bbr.2009.03.004.

Koschke, M., Boettger, M. K., Schulz, S., Berger, S., Terhaar, J., Voss, A., Yeragani, V. K., Bar, K. J., 2009. Autonomy of autonomic dysfunction in major depression. Psychosom. Med. 71(8), 852-860. https://doi.org/10.1097/PSY.0b013e3181b8bb7a.

Kreibig, S. D., 2010. Autonomic nervous system activity in emotion: a review. Biol. Psychol. 84(3), 394-421. https://doi.org/10.1016/j.biopsycho.2010.03.010.

Lajoie, G., Thivierge, J. P., Shea-Brown, E., 2014. Structured chaos shapes spike-response noise entropy in balanced neural networks. Front. Comput. Neurosci. 8, 123. https://doi.org/10.3389/fncom.2014.00123.

Lischke, A., Pahnke, R., Mau-Moeller, A., Behrens, M., Grabe, H. J., Freyberger, H. J., Hamm, A. O., Weippert, M., 2018. Inter-individual Differences in Heart Rate Variability Are Associated with Inter-individual Differences in Empathy and Alexithymia. Front. Psychol. 9, 229. https://doi.org/10.3389/fpsyg.2018.00229.

Loas, G., Fremaux, D., Marchand, M. P., 1995. [Factorial structure and internal consistency of the French version of the twenty-item Toronto Alexithymia Scale in a group of 183 healthy probands]. Encephale 21(2), 117-122.

McCraty, R., Atkinson, M., Tiller, W. A., Rein, G., Watkins, A. D., 1995. The effects of emotions on short-term power spectrum analysis of heart rate variability. Am. J. Cardiol. 76(14), 1089-1093. https://doi.org/10.1016/s0002-9149(99)80309-9.

Morin, A. J., Moullec, G., Maiano, C., Layet, L., Just, J. L., Ninot, G., 2011. Psychometric properties of the Center for Epidemiologic Studies Depression Scale (CES-D) in French clinical and nonclinical adults. Rev. Epidemiol. Sante Publique 59(5), 327-340. https://doi.org/10.1016/j.respe.2011.03.061.

Mourot, L., Bouhaddi, M., Perrey, S., Cappelle, S., Henriet, M. T., Wolf, J. P., Rouillon, J. D., Regnard, J., 2004. Decrease in heart rate variability with overtraining: assessment by the Poincare plot analysis. Clin. Physiol. Funct. Imaging 24(1), 10-18. https://doi.org/10.1046/j.1475-0961.2003.00523.x.

Muhtadie, L., Koslov, K., Akinola, M., Mendes, W. B., 2015. Vagal flexibility: A physiological predictor of social sensitivity. J. Pers. Soc. Psychol. 109(1), 106-120. https://doi.org/10.1037/pspp0000016.

Nagai, Y., Critchley, H. D., Featherstone, E., Trimble, M. R., Dolan, R. J., 2004. Activity in ventromedial prefrontal cortex covaries with sympathetic skin conductance level: a physiological account of a "default mode" of brain function. NeuroImage 22(1), 243-251. https://doi.org/10.1016/j.neuroimage.2004.01.019.

Ondicova, K., Mravec, B., 2010. Multilevel interactions between the sympathetic and parasympathetic nervous systems: a minireview. Endocr. Regul. 44(2), 69-75. https://doi.org/10.4149/endo_2010_02_69.

Ozawa, S., Kanayama, N., Hiraki, K., 2019. Emotion-related cerebral blood flow changes in the ventral medial prefrontal cortex: An NIRS study. Brain. Cogn. 134, 21-28. https://doi.org/10.1016/j.bandc.2019.05.001.

Park, G., Thayer, J. F., 2014. From the heart to the mind: cardiac vagal tone modulates top-down and bottom-up visual perception and attention to emotional stimuli. Front. Psychol. 5, 278. https://doi.org/10.3389/fpsyg.2014.00278.

Park, G., Van Bavel, J. J., Vasey, M. W., Thayer, J. F., 2013. Cardiac vagal tone predicts attentional engagement to and disengagement from fearful faces. Emotion 13(4), 645-656. https://doi.org/10.1037/a0032971.

Pilant, M., 2020. http://www.math.tamu.edu/~Michael.Pilant/math442/Matlab/lyapunov.m.

Reiter, R. J., Rosales-Corral, S., Sharma, R., 2020. Circadian disruption, melatonin rhythm perturbations and their contributions to chaotic physiology. Adv. Med. Sci. 65(2), 394-402. https://doi.org/10.1016/j.advms.2020.07.001.

Rolls, E. T., 2019. The orbitofrontal cortex and emotion in health and disease, including depression. Neuropsychologia 128, 14-43. https://doi.org/10.1016/j.neuropsychologia.2017.09.021.

Roth, T., 2009. Slow wave sleep: does it matter? J. Clin. Sleep Med. 5(2 Suppl), S4-5. https://doi.org/10.5664/jcsm.5.2S.S4.

Schafer, T., Schwarz, M. A., 2019. The Meaningfulness of Effect Sizes in Psychological Research: Differences Between Sub-Disciplines and the Impact of Potential Biases. Front. Psychol. 10, 813. https://doi.org/10.3389/fpsyg.2019.00813.

669 Scherer, K. R., 2009. Emotions are emergent processes : They require a dynamic computational
670 architecture. Philosophical Transactions of the Royal Society B: Biological Sciences
671 364(1535), 3459-3474. https://doi.org/10.1098/rstb.2009.0141.
672 Sgoifo, A., Carnevali, L., Alfonso Mde, L., Amore, M., 2015. Autonomic dysfunction and heart
673 rate variability in depression. Stress 18(3), 343-352.
674 https://doi.org/10.3109/10253890.2015.1045868.
675 Spielberger, C. D., 1983. Manual for the State-Trait-Anxiety Inventory: STAI (form Y). Palo
676 Alto, CA, USA: Consulting Psychologists Press.
677 Tarnopolski, M., 2016. On the relationship between the Hurst exponent, the ratio of the mean
678 square successive difference to the variance, and the number of turning points. Physica
679 A: Statistical Mechanics and its Applications 461, 662-673.
680 https://doi.org/10.1016/j.physa.2016.06.004.
681 Tarnopolski, M., 2018. Correlation between the Hurst exponent and the maximal Lyapunov
682 exponent: Examining some low-dimensional conservative maps. Physica A: Statistical
683 Mechanics and its Applications 490, 834-844.
684 https://doi.org/10.1016/j.physa.2017.08.159.
685 Taylor, P. A., Gohel, S., Di, X., Walter, M., Biswal, B. B., 2012. Functional covariance
686 networks: obtaining resting-state networks from intersubject variability. Brain Connect.
687 2(4), 203-217. https://doi.org/10.1089/brain.2012.0095.
688 Thayer, J. F., Lane, R. D., 2009. Claude Bernard and the heart-brain connection: further
689 elaboration of a model of neurovisceral integration. Neurosci. Biobehav. Rev. 33(2), 81-
690 88. https://doi.org/10.1016/j.neubiorev.2008.08.004.
691 Udupa, K., Sathyaprabha, T. N., Thirthalli, J., Kishore, K. R., Lavekar, G. S., Raju, T. R.,
692 Gangadhar, B. N., 2007. Alteration of cardiac autonomic functions in patients with major
693 depression: a study using heart rate variability measures. J. Affect. Disord. 100(1-3), 137-
694 141. https://doi.org/10.1016/j.jad.2006.10.007.
695 von Holzen, J. J., Capaldo, G., Wilhelm, M., Stute, P., 2016. Impact of endo- and exogenous
696 estrogens on heart rate variability in women: a review. Climacteric 19(3), 222-228.
697 https://doi.org/10.3109/13697137.2016.1145206.
698 Wan, J. (Writer). (2013). The Conjuring In. North Carolina. USA: New Line Cinema.
699 Willroth, E. C., Flett, J. A. M., Mauss, I. B., 2020. Depressive symptoms and deficits in stress-
700 reactive negative, positive, and within-emotion-category differentiation: A daily diary
701 study. J. Pers. 88(2), 174-184. https://doi.org/10.1111/jopy.12475.
702 Yeragani, V. K., Rao, R., Jayaraman, A., Pohl, R., Balon, R., Glitz, D., 2002. Heart rate time
703 series: decreased chaos after intravenous lactate and increased non-linearity after
704 isoproterenol in normal subjects. Psychiatry Res. 109(1), 81-92.
705 https://doi.org/10.1016/s0165-1781(01)00355-9.
706 Young, H., Benton, D., 2015. We should be using nonlinear indices when relating heart-rate
707 dynamics to cognition and mood. Sci. Rep. 5, 16619. https://doi.org/10.1038/srep16619.
708

6. Author notes

6.1. Acknowledgements

The authors thank SCREEN (*service commun de ressources d'expérimentation et d'équipement numérique*) for making their platform (MSH-Alpes Grenoble, Maison des Sciences de l'Homme) available for this study.

6.2. Funding

Grants from the Délégation Générale à l'Armement (DGA) supported the study.

6.3. Competing interests

The authors declare no competing interests.

The opinions or assertions expressed here are the private views of the authors and are not to be considered as official or as reflecting the views of the French Military Health Service.

6.4. Data and material availability

All algorithms and the video are available on reasonable request from the corresponding author.